Multiple stressors threaten an important coastal foundation species

Running head: Interacting stressors reduce eelgrass

Jonathan S. Lefcheck[1*], David J. Wilcox[1], Rebecca R. Murphy[2], Scott R. Marion[3], Robert J. Orth[1]

[1]Virginia Institute of Marine Science, The College of William & Mary, Gloucester Point, VA 23062, USA

[2]University of Maryland Center for Environmental Science, Chesapeake Bay Program, Annapolis, MD 21403, USA

[3]Oregon Department of Fish & Wildlife, Marine Resources Program, Newport, OR 97365, USA

[*]Corresponding author. Email: jslefche@vims.edu. Phone: +1 804 684 7150. Mailing address: PO Box 1346, Gloucester Point, VA 23062, USA

Keywords: eelgrass, seagrass, climate change, eutrophication, remote sensing, Chesapeake Bay

Type of paper: Primary Research Article

Abstract

Interactions among global change stressors and their effects at large scales are often proposed but seldom evaluated, in part due to lack of comprehensive, sufficiently long-term, and spatially-extensive datasets. Seagrasses, which provide nursery habitat, improve water quality, and constitute a globally-important carbon sink, are among the most vulnerable habitats on the planet. Here, we unite 31-years of high-resolution aerial monitoring and water quality data to elucidate the patterns and drivers of eelgrass (*Zostera marina*) abundance in Chesapeake Bay, USA, one of the largest and most valuable estuaries in the world, with an unparalleled history of regulatory efforts. We show that eelgrass cover has declined 29% in total since 1991, with wide-ranging and severe ecological and economic consequences. We go on to identify an interaction between decreasing water clarity and warming temperatures as the primary driver of this trend. Declining clarity has gradually reduced eelgrass over the past two decades, primarily in deeper beds where light is already limiting. In shallow beds, however, reduced visibility exacerbates the physiological stress of acute warming, leading to recent instances of decline approaching 80%. While degraded water quality has long been known to influence underwater grasses worldwide, we demonstrate a clear and rapidly emerging interaction with climate change. We highlight the urgent need to integrate a broader perspective into local water quality management, in the Chesapeake Bay and in the many other coastal systems facing similar stressors.

PeerJ Preprints | https://doi.org/10.7287/peerj.preprints.2544v1 | CC BY 4.0 Open Access | rec: 21 Oct 2016, publ: 21 Oct 2016

Introduction

Identifying the drivers of environmental change and predicting their consequences is the preeminent scientific challenge of the Anthropocene (Halpern *et al.*, 2008). Marine systems in particular are experiencing rapid and often irreversible alterations as a consequence of human activities (Lotze *et al.*, 2006), and almost half of these changes can be attributed to multiple drivers (Lotze *et al.*, 2006; Halpern *et al.*, 2008). Despite the increasing recognition that global and local stressors often act jointly, rigorous empirical examples of this phenomenon are lacking at the large scales relevant to both the observed change and human well-being, particularly in temperate ecosystems where most of the world's human population reside. Instead, most of our understanding comes from small-scale experiments and observations (Crain *et al.*, 2008, 2009), or from tropical systems such as coral reefs (Gardner *et al.*, 2003; De'ath *et al.*, 2012). This knowledge gap vastly impedes our ability to predict and avert the impacts of global change, particularly given the fact that stressors, and corresponding management actions, occur at much larger scales.

Seagrasses in particular are extremely sensitive to global change, with losses exceeding 25% worldwide in just the last century (Orth *et al.*, 2006; Waycott *et al.*, 2009). Because of its global distribution close to major anthropogenic influences, and its habit of forming monospecific stands in shallow zones, eelgrass (*Zostera marina*) is acutely vulnerable to environmental stressors (Waycott *et al.*, 2009). Consequently, it has experienced declines in many locations, including in northern Europe (Giesen *et al.*, 1990; Frederiksen *et al.*, 2004), the northwestern Atlantic (Beem & Short, 2009; Costello & Kenworthy, 2011), and the western coast of the US, particularly San Francisco Bay (Short & Wyllie-Echeverria, 1996) , but nowhere has it experienced more significant losses than in Chesapeake Bay, USA (Orth & Moore, 1983).

The Chesapeake Bay is one of the largest, most well-managed, and economically productive coastlines in the world, and is projected to support 20 million people by 2020 (Claggett, 2016).

PeerJ Preprints | https://doi.org/10.7287/peerj.preprints.2544v1 | CC BY 4.0 Open Access | rec: 21 Oct 2016, publ: 21 Oct 2016

While the abundance of eelgrass in Chesapeake Bay is known to have fluctuated over the last century due to storms and a wasting disease (Orth & Moore, 1983; Orth *et al.*, 2010), it was a single summer in 1972 that Tropical Storm Agnes extirpated over 50% of the population from which Chesapeake Bay has never recovered (Fig. 1). While several studies have hypothesized that declining water quality may be preventing recovery of eelgrass in Chesapeake Bay (Orth *et al.*, 2010; Patrick & Weller, 2015), and indeed may be driving its continued decline, the environmental drivers of this valuable habitat have yet to be confidently enumerated. In this study, we use 31-years of high-resolution aerial imagery and water quality data to document the continued decline of eelgrass in Chesapeake Bay, and directly link changes in its distribution to multiple anthropogenic stressors. The scale, duration, comprehensiveness, and complementarity of these two datasets are unprecedented, and provide a unique opportunity to understand the specific drivers of habitat decline in highly populated coastal systems.

Methods

Submersed Aquatic Vegetation Monitoring

Submersed aquatic vegetation (SAV) bed area and percent cover was derived from aerial imagery acquired on an annual basis from 1984 through 2015, except for 1988, from the Virginia Institute of Marine Science SAV Monitoring Program (http://www.vims.edu/bio/sav). Panchromatic photography at a scale of 1:24,000; 60% flightline overlap and 20% sidelap was acquired with a standard mapping camera for 1984 – 2014. Multi-spectral imagery was acquired in 2014 and 2015 using a digital mapping camera with a ground sample distance of 24 cm. Acquisition conditions, including tidal stage, plant growth, sun angle, atmospheric transparency, water turbidity, and wind, were selected to optimize the visibility of seagrass beds (Dobson *et al.*, 1995).

Mapping of seagrass beds was initially accomplished by manually tracing seagrass bed outlines on to translucent United States Geological Survey 7.5-minute quadrangle maps directly

PeerJ Preprints | https://doi.org/10.7287/peerj.preprints.2544v1 | CC BY 4.0 Open Access | rec: 21 Oct 2016, publ: 21 Oct 2016

from the photographs, and then digitizing bed boundaries into a Geographic Information System (GIS) dataset for analysis. More recently, the aerial photography was scanned from negatives or produced digitally from the sensor and ortho-rectified using ERDAS LPS image-processing software (ERDAS, Atlanta GA). SAV bed boundaries were then photo-interpreted directly on-screen while maintaining a fixed scale using ESRI ArcMap GIS software (ESRI, Redlands CA).

Water Quality Monitoring

Water quality data were obtained from the Chesapeake Bay Program's (CBP) Water Quality Database (http://www.chesapeakebay.net), which contains data collected in the tidal waters of Chesapeake Bay by agencies including Maryland Department of Nature Resources and Virginia Department of Environmental Quality. The program visits approximately 160 fixed monitoring stations every two weeks, 28 of which were used for our analysis (Fig. S2). At each station, a vertical hydrographic profile is collected using a multiparameter sonde with observations every 1-2 meters of water temperature, specific conductivity (to calculate salinity), and dissolved oxygen. Secchi depth is observed in the field using a black-and-white Secchi disk attached to a measuring line. In addition, at each station, water samples are collected at several depths and processed at a laboratory to quantify concentrations of chlorophyll-*a*, total nitrogen, and total phosphorus. For this analysis, we used data only from the surface layer, the top 0.5 or 1 m observation, assuming these values most reflect conditions in the shallow water where eelgrass is present.

Methodological changes for chlorophyll-*a*, total nitrogen, and total phosphorus over the course of the survey necessitated the implementation of a correction factors. Specifically, for nitrogen, the changes involved switching from a sum of nitrate, nitrite, and total Kjeldahl nitrogen to total dissolved nitrogen plus particulate nitrogen at Virginia mainstem stations in 1988, Maryland stations in 1998 and Virginia tributary stations in 1998. For phosphorus, the change involved switching from a sum of total dissolved phosphorus plus particulate phosphorus to a

PeerJ Preprints | https://doi.org/10.7287/peerj.preprints.2544v1 | CC BY 4.0 Open Access | rec: 21 Oct 2016, publ: 21 Oct 2016

direct measurement in the same years as the total nitrogen changes. For chlorophyll-*a*, the possible changes occurred due to laboratories switches in the late 1990s, although it is likely this only impacted Virginia tributary stations. For these three variables, we regressed the response at each station against the identity of the processing laboratory and the method employed using simple linear regression. We then extracted the residuals from this relationship, and visual assessment of time series plots suggested that they adequately accounted for the *a priori* influence of lab and method. The residuals for these three variables were carried through all subsequent analyses.

While these stations are primarily in deep water, many prior studies have shown that they can be adequately extrapolated to predict underwater vegetation in shallow areas (Li *et al.*, 2007; Rybicki & Landwehr, 2007; Ruhl & Rybicki, 2010; Gurbisz & Kemp, 2014; Patrick *et al.*, 2014, 2016). Even if the stations under- or over-represent conditions at shallow depths, the relative differences among stations and years are preserved, such that any inferences about the directionality and relative impact of the environmental variables should be unaffected.

Statistical Analysis

A cell-based model with a cell size of 30 m was used to facilitate the analysis. Within the study area, ESRI ArcGIS software was used to code each 30 m cell in one of the following categories on the Braun-Blanquet cover scale: none (0% cover), very sparse (<10% cover), sparse (11-40% cover), moderate (41-70%), or dense (71-100%) (Paine, 1981). Additionally, we quantified the depth of the cell extracted from the Chesapeake Bay, VA/MD (M130) Bathymetric Digital Elevation Model (NOAA, http://estuarinebathymetry.noaa.gov/). For each grid cell, we then calculated the over-water distance to the nearest CBP monitoring station, and grouped all cells based on their nearest station, which we refer to as 'subregions' (Fig. S2). For each station, we calculated the total eelgrass cover as the sum of the cover of the nearest grid cells, weighted by the Braun-Blanquet

PeerJ Preprints | https://doi.org/10.7287/peerj.preprints.2544v1 | CC BY 4.0 Open Access | rec: 21 Oct 2016, publ: 21 Oct 2016

density to yield a value of total bottom area covered, and merged these with the environmental data. This procedure yielded n = 684 observations for use in our modelling exercise.

We used the following generalized additive mixed model to identify the significant predictors of eelgrass cover:

$$y_{ij} = \boldsymbol{X}_{ij} * \alpha + \sum_{k=1}^{p} f_k(x_{ij}) + \boldsymbol{Z}_{ij} b_{ij} + \boldsymbol{Z}_{i,j} \boldsymbol{b_i} + \epsilon_{ij}$$

$$\boldsymbol{b_i} = N(\boldsymbol{0}, \boldsymbol{\Psi}_1)$$

$$b_{ij} = N(0, \sigma_2^2)$$

$$\epsilon_{ij} = N(\boldsymbol{0}, \sigma^2 \boldsymbol{I})$$

where the response y_{ij} is the $\log_{10}$-transformed density-weighted total cover of eelgrass in subregion i in year j, $\boldsymbol{X}_{ij}$ is the design matrix of parametric components and α is the vector of fixed effects parameters, $f_k(\cdot)$ are the non-parametric smoothed functions of covariates x_{ij}, $\boldsymbol{Z}_{ij}$is the design matrix of the random effect of subregion i in year j and b_{ij} is the corresponding vector of random effects, $\boldsymbol{Z}_{i,j}$ is the design matrix of the random effect of year j on the measurements for subregion i in year j and $\boldsymbol{b_i}$ is the corresponding vector of random effects, and ϵ_{ij} is the within-subregion and within-year error independent of the random effects. All random effects and residual error are assumed to be normally distributed with a mean of 0, and positive definite variance-covariance matrices $\boldsymbol{\Psi}_1$, σ_2^2, and $\sigma^2 \boldsymbol{I}$.

For the non-parametric component:

$$\sum_{k=1}^{p} f_k(x_{ij}) = f_1(\text{Long, Lat}) + f_2(\text{Cover}_{\text{i(j}-1)}) + f_3(\text{Habitat}_i) + f_4(\text{Chl}a_{ij}) + f_5(\text{Salinity}_{ij})$$
$$+ f_6(\text{Secchi}_{ij}) + f_7(\text{TN}_{ij}) + f_8(\text{TP}_{ij}) + f_9(\text{Temp}_{i(j-1)}) + f_{10}(\text{MaxTemp}_{i(j-1)})$$
$$+ f_{11}(\text{Secchi}_{ij}, \text{Temp}_{i(j-1)})$$

PeerJ Preprints | https://doi.org/10.7287/peerj.preprints.2544v1 | CC BY 4.0 Open Access | rec: 21 Oct 2016, publ: 21 Oct 2016

where all predictors are modeled as smoothing functions using the default thin-plate regression spline in the *mgcv* package in R (Wood, 2011). $f_1(\text{Long, Lat})$ is a smoothed combination of spatial coordinates using the UTM projection, and is meant to address any potential spatial autocorrelation among the subregions. $f_2(\text{Cover}_{i(j-1)})$ represents eelgrass cover in subregion i in the previous year $j-1$, to account for the dependency of eelgrass cover from one year to the next. We fit this predictor as a smoothed covariate in lieu of a fixed autoregressive structure, having tested various combinations using model comparisons and visual examination of (partial) residual autocorrelation functions, and finding them to be less supported than simply modeling the previous year's eelgrass cover. $f_3(\text{Habitat}_{ij})$ represents the total available bottom for eelgrass with subregion i extending to 1 m Mean Low Water.

The remaining predictors are environmental variables summarized from the CBP Monitoring Program. Chlorophyll-*a*, salinity, Secchi depth, total nitrogen (TN), and total phosphorus (TP) were calculated as means for February to June in subregion i of year j, as we expected eelgrass to respond most strongly to these parameters during the growing season. The two predictors pertaining to temperature, $f_9(\text{Temp}_{i(j-1)}) + f_{10}(\text{MaxTemp}_{i(j-1)})$, were calculated as the mean and maximum values, respectively, from July to September of the previous year $j-1$, since this is the time during which eelgrass undergoes natural temperature-driven senescence in this region (Moore & Jarvis, 2008). The final term is a combination of mean temperature and Secchi depth, estimating their interactive influence on cover independent of their main effects using a tensor product moment interaction smoother.

The model was constructed in R version 3.3.1 (R Development Core Team, 2016) using the *mgcv* package (Wood, 2011). The model was fit using restricted maximum likelihood (REML) to avoid overfitting and yield less biased estimates of the fixed effects, given the complexity of the model and the size of the dataset. Model assumptions of normality of errors and constant variance

PeerJ Preprints | https://doi.org/10.7287/peerj.preprints.2544v1 | CC BY 4.0 Open Access | rec: 21 Oct 2016, publ: 21 Oct 2016

were assessed visually. Model predictions and 95% confidence intervals were obtained using the custom function *EvaluateSmooths* modified from[1], and from a modified version of the function *pvisgam* in the *itsadug* package (van Rij *et al.*, 2016). We held a Type I error threshold of $\alpha = 0.05$. All data and scripts necessary to reproduce the analyses and generate all graphics are provided as supplementary files.

Ecosystem Services and Valuation

To estimate the potential ecological and economic losses associated with the decline of eelgrass, we collated *in situ* measurements of functioning from Chesapeake Bay eelgrass beds of the last decade (Table 1).

Data for estimation of total carbon loss were derived from in situ measurements of carbon stock as part of the Zostera Experimental Network (http://zenscience.org). Sediment core tubes (length: 50 cm, diameter: 50 mm) were forced to a depth of 30-40 cm into the sediment at a minimum distance of 15 m from each other at Goodwin Island, York River, extracted, and returned to the laboratory on ice. The samples were then dried and shipped to University of Southern Denmark, where samples were analyzed for sediment δ^{13} C, δ^{15} N, PON and POC using a mass spectrometer (Thermo Scientific, delta V advantage, isotope ratio mass spectrometer). The measured isotope ratios were represented using the δ- notation with Vienna Peedee belemnite as reference material. Values of POC obtained by depth integration of the carbon density (mg C cm^{-3}) of 0-25 cm sediment layers were converted to carbon stock per unit sediment (mg C cm^{-2}), and averaged across n = 3 samples. We then averaged across all samples to yield a mean and standard deviation.

[1] https://stackoverflow.com/questions/19735149/is-it-possible-to-plot-the-smooth-components-of-a-gam-fit-with-ggplot2

PeerJ Preprints | https://doi.org/10.7287/peerj.preprints.2544v1 | CC BY 4.0 Open Access | rec: 21 Oct 2016, publ: 21 Oct 2016

Estimates of N_2 fixation were obtained from (Cole, 2011), which reports estimates of whole system nitrogen flux, including the plant itself, epiphytes, and the sediment. In the publication, the author reports N_2 fixation rates as 3.9-5.8 g N m^{-2} y^{-1}. From this range, we obtained an average by taking the difference and dividing by two, and adding it to the lesser value, yielding 4.85 g N m^{-2} y^{-1}.

Estimates of epifaunal invertebrate biomass per unit area were obtained from a long-running field survey at Goodwin Island, York River, Chesapeake Bay from 2004-2012 (Douglass *et al.*, 2010). Ten grab samples per month collected epifauna over an area equivalent to 400 cm^2 of bottom. Animals in each sample were size fractionated and biomass was estimated in mg ash-free dry mass using linear equations in (Edgar, 1990). These values were then averaged across all months and years to produce a mean and standard errors.

Juvenile blue crab abundance per unit area was obtained from (Ralph *et al.*, 2013). Values were averaged across all sampling locations to yield approximately 24 individuals m^{-2}, and standard deviations derived from standard error of the mean multiplied by the square root of the total sample size. A market price of $US 3418 per metric ton was obtained from NOAA Office of Science and Technology Annual Commercial Landing Statistics (NOAA Office of Science and Technology, 2014) for the most recent available year (2014), including both hard- and soft-shelled individuals. We assumed an average adult mass of 150 g, and a conservative 10% catchability arising from a combination of post-juvenile mortality and fishing effort.

Estimates of silver perch production were obtained from (Sobocinski & Latour, 2015). We used a mean value of 91.5 g m^{-2} y^{-1}, and obtained standard errors from the range 77.8-117.8 g m^{-2} y^{-1} using the range rule, as above. Information on the fishery harvest of approximately 5900 mt y^{-1} from the period of 2004-2014 also came from (Sobocinski & Latour, 2015).

Finally, estimates of total economic loss were obtained from (Costanza *et al.*, 2014), and as with all of the above estimates, assumes a 'basic benefit transfer' implying that the value of the

PeerJ Preprints | https://doi.org/10.7287/peerj.preprints.2544v1 | CC BY 4.0 Open Access | rec: 21 Oct 2016, publ: 21 Oct 2016

service remains consistent per unit area. These values integrate across a range of potentially economically valuable services including provisioning of food and materials, bioprospecting, regulation of air, water, and climate, nursery services, and cultural, recreational and spiritual benefits (de Groot *et al.*, 2012). We used the 2011 valuation of \$28,916 ha^{-1} y^{-1} for combined seagrass/algal beds, noting that seagrass beds often accumulate vast quantities of macroalgae.

For all values, we extrapolated to the total area lost multiplied by the period of time considered (30 years, if to present, or 22, if to the greatest observed loss). For nitrogen fixation and silver perch production, standard deviations were approximated by taking the difference of the range and dividing by 4, or the 'range rule.'

Results

From a peak in 1991, representing the maximum recovery post-Agnes, total eelgrass cover has declined by 29% to date (Fig. 2A). Moreover, the mean depth of eelgrass beds has declined by 0.12 m, or 26%, with the majority of change occurring abruptly in 1997 (Fig. 2B). This change represents a greater loss of deep beds, which were reduced by 50%, versus shallow beds, which actually increased in cover by 35% (Fig. 2C). Eelgrass beds have therefore shifted 165 m closer to shore since 1984 (Fig. 2C). Together, these results depict a 'habitat squeeze,' with eelgrass retreating into shallow water refugia where conditions are still favorable for growth, and all but eliminated in many areas >0.5 m depth where it was once abundant.

The widespread decline in eelgrass cover after 1991 appears to have been gradual until the early 2000s, after which point several acute diebacks occurred (Fig. 2A). The most extreme loss occurred in 2006, with a catastrophic 58% decline from the previous year, and a 78% decline from peak cover. Interestingly, eelgrass appeared to recover rapidly after these declines. Following the 2006 die-back, eelgrass cover increased by 55% over the previous year, and by 2009, had reached cover exceeding that observed immediately prior to the die-back. A similar scenario occurred in

PeerJ Preprints | https://doi.org/10.7287/peerj.preprints.2544v1 | CC BY 4.0 Open Access | rec: 21 Oct 2016, publ: 21 Oct 2016

2011, where a less severe but still substantial decline of 41% reached pre-die-back cover in less than two years. Our observations suggest eelgrass is responding to multiple drivers, one halting its recovery in the early 1990s and impacting eelgrass over the longer term, and another, more episodic driver beginning in the mid-2000s that relaxes enough to permit rapid recovery.

To clarify the correlates of eelgrass cover, we constructed a generalized additive mixed model (GAMM) incorporating 10 spatial, temporal, and environmental variables that together explained 84.6% of the variance in eelgrass cover. Beyond the expected influence of space and time, Secchi depth (an indicator of water clarity), mean water temperature of the preceding summer, and their interaction were the only other significant predictors of eelgrass cover ($P = 0.006$ and $P < 0.001$, $P = 0.029$, Fig. 3).

Decreasing Secchi depth (i.e., reduced clarity) is predicted to reduce eelgrass cover (Fig. 3A), and has declined by 30 cm since the beginning of the survey (Fig. 3B). Light is the principal factor governing eelgrass growth (Dennison, 1987), and our analysis confirms the long-running hypothesis that reduced water clarity is driving the long-term decline of eelgrass in Chesapeake Bay (Michael Kemp *et al.*, 2004; Orth *et al.*, 2010), and in many other locations (Giesen *et al.*, 1990; Short & Wyllie-Echeverria, 1996). It also explains why deep beds have exhibited the strongest decline (Fig. 2C), as light penetration decreases exponentially with depth (Dennison, 1987). To confirm this, we re-fit GAMMs for each depth strata, and show that Secchi depth is the only significant predictor of eelgrass cover at depths >0.5 m ($P = 0.02$, Fig. S1).

Increasing mean summer temperatures also reduced eelgrass cover, but only when exceeding ≈25°C (Fig. 3C), a well-described threshold for mortality in this species (Reusch *et al.*, 2005). Not only has the average summertime temperature increased from 24.9 to 26.4°C since 1984, but the frequency of extreme mean temperatures (>28°C) has doubled in the last decade (Fig. 3D), generalizing recent conclusions about the role of episodic heat events in driving localized

PeerJ Preprints | https://doi.org/10.7287/peerj.preprints.2544v1 | CC BY 4.0 Open Access | rec: 21 Oct 2016, publ: 21 Oct 2016

diebacks (Moore & Jarvis, 2008). Thus, warming is the most likely candidate behind more recent declines (Fig. 2A), particularly in shallow waters where light is not limiting (Fig. 2C). Indeed, GAMMs fit to individual depth strata show a significant effect of temperature only at intermediate and shallow depths (0-5 m, $P = 0.008$ and $P = 0.04$, Fig. S1).

Most importantly, we show that temperature and clarity interactively reduce eelgrass cover beyond what is expected from either alone (Fig. 2c, d, Fig. 4). A 2°C increase in temperature, which is the low end of expectations for the Chesapeake Bay in the next 30 years (Najjar *et al.*, 2010), would result in a further decline of 38%, holding all else constant. Similarly, if Secchi depth continues on its trajectory and is reduced by another 40% over the next 30 years, it would result in a further decline of 84%. However, combined changes in temperature and Secchi depth would result in an expected loss of 95%, or the near total eradication of eelgrass in the Chesapeake Bay. While these values are based only on our model, and do not integrate any biology or take into account continued management actions to reduce inputs into the Bay, it demonstrates potential for catastrophic losses as a result of the joint influence of these two stressors.

Finally, from independent *in situ* measurements in Chesapeake Bay eelgrass beds, we show loss of eelgrass has likely had severe consequences for ecosystem functioning and the provision of services relevant to human well-being (Table 1). For example, the total loss of carbon in sediments is estimated at 693-1859 kt C. Given the current social cost of carbon (Domestic Policy Council, 2013), this equates to an expected economic loss of $US 96.5 – 259 million. Similarly, loss of eelgrass is expected to lead to a reduction of 523-1403 million juvenile blue crabs. Assuming a conservative 10% harvestable yield and the 2014 market price (NOAA Office of Science and Technology, 2014), this equates to a total potential economic loss of $US 28.6 – 76.7 million, which is 1-2 years of the fishery. Similarly, the expected loss of silver perch equates to 10-20 years of the fishery (Sobocinski & Latour, 2015). In all, an independent and integrated measure of economic

PeerJ Preprints | https://doi.org/10.7287/peerj.preprints.2544v1 | CC BY 4.0 Open Access | rec: 21 Oct 2016, publ: 21 Oct 2016

valuation (Costanza *et al.*, 2014) places the total potential economic loss as a consequence of the decline of eelgrass in Chesapeake Bay at $US 1.51-2.54 billion.

Although these values are estimates extrapolated from small-scale data uninformed by the well-described variation in these services through time and space (Duffy *et al.*, 2015), and therefore must be interpreted with caution, they represent the best available data for assessing the outcome of eelgrass decline for the ecological and economic well-being of the Chesapeake Bay.

Discussion

Since the early 1990s, we show that eelgrass abundance in Chesapeake Bay has undergone a steady deterioration, punctuated by periods of intense decline (Fig. 2a). We propose that the long-term declines are a consequence of declining water clarity, and has all but eliminated eelgrass beds deeper than 1 m where light is already limiting (Fig. 2c, Fig. S1). As the influence of clarity was independent of nutrients or chlorophyll-*a* in our model, we propose that its effect stems from increased sediment loading, resuspension, and dissolution of organic matter due to greater watershed development and urbanization (Gallegos, 2001; Michael Kemp *et al.*, 2004). At the same, we demonstrate that increasing summertime temperatures are likely behind episodic declines in 2005 and 2010, but are sufficiently sporadic to allow recovery (Fig. 2a). Critically, high temperatures appear to impact shallow beds more than deep ones (Fig. S2), suggesting that warming, and its interaction with clarity, is the most prominent threat for remaining eelgrass in Chesapeake Bay.

Warming has two implications for the persistence of eelgrass in Chesapeake Bay. First, it has been shown that rising temperatures elevates respiratory load, increasing light requirements for photosynthesis to balance metabolic demand, and exacerbating the negative effects associated with decreasing clarity (Moore *et al.*, 2012). Consistent with this hypothesis, we show a highly significant interaction between the two such that the strongest declines are expected when

PeerJ Preprints | https://doi.org/10.7287/peerj.preprints.2544v1 | CC BY 4.0 Open Access | rec: 21 Oct 2016, publ: 21 Oct 2016

317 temperature is maximal and Secchi depth is at its minimum (Fig. 4). Second, eelgrass propagates
318 both sexually, via seeds, and asexually, via clonal growth. When local populations die-back as a
319 consequence of heat stress, the seedbank from the previous year permits rapid recolonization.
320 However, diebacks in two consecutive years would eliminate the seedbank, as eelgrass seedlings
321 flower in the second year of growth, excluding any possibility of recovery (Jarvis & Moore, 2010).

322 While eelgrass has stalled on its track of recovery since 1991, over the short-term it has
323 actually increased in abundance (Fig. 2A). We note, however, that cover observed at any point
324 during this survey is only a fraction of what it was prior to the 1970s (Fig. 1), and more critically, is
325 now restricted to only the most nearshore areas (Fig. 2C). Losses prior to this survey are also
326 known to have come from pulse events, namely storms and disease, and have generally recovered
327 within a decade or two (Orth & Moore, 1983; Orth *et al.*, 2010). In contrast, we demonstrate a
328 strong anthropogenic component in driving the continued and contemporary decline of eelgrass
329 through degradations in water quality, warming, and their interaction. Therefore, we temper
330 optimism of this recent upswing, and caution that without continued intervention to mitigate
331 human impacts, principally those that affect light availability, eelgrass is unlikely to even reach
332 coverage observed in the early 1990s, let alone historical maximums. This point is critical
333 considering those maximums have been used to set management targets for cover of underwater
334 grasses in the polyhaline region of the Bay (Orth *et al.*, 2010).

335 Our study contributes to a general pattern of fragility among coastal ecosystems for which
336 long-term regional records exist, including the Great Barrier and Caribbean coral reefs (Gardner *et*
337 *al.*, 2003; De'ath *et al.*, 2012), kelp forests (Wernberg *et al.*, 2016), salt marshes (Jefferies *et al.*,
338 2006), and mangroves (Fromard *et al.*, 2004; Cavanaugh *et al.*, 2014). It also provides the most
339 spatially and temporally comprehensive assessment of the patterns and drivers of decline in any
340 seagrass species, and for one the largest, most productive, and valuable estuaries in the world
341 (Claggett, 2016). Most importantly, we generalize mechanisms of seagrass decline derived from

PeerJ Preprints | https://doi.org/10.7287/peerj.preprints.2544v1 | CC BY 4.0 Open Access | rec: 21 Oct 2016, publ: 21 Oct 2016

small-scale experiments and local observations to the scale of the entire Chesapeake Bay, principally sensitivity to declining water clarity and physiological intolerance to warming temperatures, as well as their interaction. This finding suggests that these mechanisms may be scale invariant, and that experiments conducted in other systems could be reasonably extrapolated to predict regional abundance of eelgrass elsewhere (Reusch *et al.*, 2005).

Instead of facilitating decline, as we demonstrate here, climate change has been shown to mediate turnover in foundational species, for example the replacement of marshes by mangroves in the southeastern US (Cavanaugh *et al.*, 2014). In contrast with our study, there is no obvious candidate to supplant eelgrass in the Chesapeake Bay. Only one underwater grass coexists with eelgrass in the region, widgeongrass (*Ruppia maritima*), but it is generally restricted to shallow waters and so far has failed to establish in any abundance in areas vacated by eelgrass (Orth *et al.*, 2010). Rather, lost beds have by and large reverted to bare sediment, the least productive marine habitat (Duarte & Cebrián, 1996). Thus, the current crisis for eelgrass in Chesapeake Bay represents an almost total loss of functionality, echoing recent findings from systems such as coral reefs, where the transition to an algal-dominated state has reduced or eliminated many of the same habitat and provisioning services (Graham & Nash, 2013).

Managers have long recognized that local-scale degradation of water clarity negatively affects many species of underwater grasses, not just eelgrass, from the Chesapeake Bay to the Gulf of Mexico, San Francisco Bay, and Australia (Giesen *et al.*, 1990; Short & Wyllie-Echeverria, 1996; Orth *et al.*, 2006; Waycott *et al.*, 2009). However, few if any implement strategies that account for rising temperatures in attempting to avert losses due to reduced water quality, despite mounting evidence of temperature-induced diebacks (Waycott *et al.*, 2009), even in places as far north as the Baltic Sea (Reusch *et al.*, 2005). This failure may explain the accelerating decline of seagrass species over the last century despite increasing awareness and intervention (Waycott *et al.*, 2009). Since climate change is a global phenomenon, we propose that managers must increase their water

PeerJ Preprints | https://doi.org/10.7287/peerj.preprints.2544v1 | CC BY 4.0 Open Access | rec: 21 Oct 2016, publ: 21 Oct 2016

quality targets at the local level to offset losses caused by global factors outside their immediate control. Indeed, our model predictions show that given sufficient water clarity, eelgrass can still persist in the face of increasing temperatures. Only by adopting such an integrative perspective can we protect and restore eelgrass in the Chesapeake Bay, and elsewhere.

Acknowledgments

We thank the US Environmental Protection Agency Chesapeake Bay Program, National Oceanic Atmospheric Administration Virginia Coastal Program, Virginia Department of Environmental Quality and Maryland Department of Natural Resources for providing funding. We thank E. Röhr and C. Boström for blue carbon data, and W. Dennison, K. Moore, D. Rasher, and J.E. Duffy for comments on previous drafts. This is contribution no. #### of the Virginia Institute of Marine Science.

References

Beem NT, Short FT (2009) Subtidal eelgrass declines in the Great Bay Estuary, New Hampshire and Maine, USA. *Estuaries and Coasts*, **32**, 202–205.

Cavanaugh KC, Kellner JR, Forde AJ, Gruner DS, Parker JD, Rodriguez W, Feller IC (2014) Poleward expansion of mangroves is a threshold response to decreased frequency of extreme cold events. *PNAS*, **111**, 723–7.

Claggett P (2016) Chesapeake Bay Program.

Cole LW (2011) *Inputs and fluxes of nitrogen in the Virginia coastal bays: Effects of newly-restored seagrasses on the nitrogen cycle*. University of Virginia, 1-129 pp.

Costanza R, de Groot R, Sutton P et al. (2014) Changes in the global value of ecosystem services. *Global Environmental Change*, **26**, 152–158.

Costello CT, Kenworthy WJ (2011) Twelve-Year Mapping and Change Analysis of Eelgrass (Zostera marina) Areal Abundance in Massachusetts (USA) Identifies Statewide Declines. *Estuaries and Coasts*, **34**, 232–242.

Crain CM, Kroeker K, Halpern BS (2008) Interactive and cumulative effects of multiple human stressors in marine systems. *Ecology Letters*, **11**, 1304–1315.

Crain CM, Halpern BS, Beck MW, Kappel C V. (2009) Understanding and managing human threats to the coastal marine environment. *Annals of the New York Academy of Sciences*, **1162**, 39–62.

De'ath G, Fabricius KE, Sweatman H, Puotinen M (2012) The 27-year decline of coral cover on the Great Barrier Reef and its causes. *PNAS*, **109**, 17995–9.

398 Dennison WC (1987) Effects of light on seagrass photosynthesis, growth and depth distribution.
399 *Aquatic Botany*, **27**, 15–26.

400 Dobson JE, Bright EA, Ferguson RL et al. (1995) *NOAA coastal change analysis program (C-CAP):*
401 *guidance for regional implementation*. US Department of Commerce, National Oceanic and
402 Atmospheric Administration, National Marine Fisheries Service.

403 Domestic Policy Council (2013) Technical Support Document:-Technical Update of the Social Cost
404 of Carbon for Regulatory Impact Analysis-Under Executive Order 12866.

405 Douglass JG, France KE, Paul Richardson J, Duffy JE (2010) Seasonal and interannual changes in a
406 Chesapeake Bay eelgrass community: Insights into biotic and abiotic control of community
407 structure. *Limnology and Oceanography*, **55**, 1499–1520.

408 Duarte CM, Cebrián J (1996) The fate of marine autotrophic production. *Limnology and*
409 *Oceanography*, **41**, 1758–1766.

410 Duffy JE, Reynolds PL, Boström C et al. (2015) Biodiversity mediates top-down control in eelgrass
411 ecosystems: a global comparative-experimental approach. *Ecology Letters*, **18**, 696–705.

412 Edgar GJ (1990) The use of the size structure of benthic macrofaunal communities to estimate
413 faunal biomass and secondary production. *Journal of Experimental Marine Biology and Ecology*,
414 **137**, 195–214.

415 Frederiksen M, Krause-Jensen D, Holmer M, Laursen JS (2004) Long-term changes in area
416 distribution of eelgrass (Zostera marina) in Danish coastal waters. *Aquatic Botany*, **78**, 167–
417 181.

418 Fromard F, Vega C, Proisy C (2004) Half a century of dynamic coastal change affecting mangrove
419 shorelines of French Guiana. A case study based on remote sensing data analyses and field
420 surveys. *Marine Geology*, **208**, 265–280.

421 Gallegos CL (2001) Calculating Optical Water Quality Targets to Restore and Protect Submersed
422 Aquatic Vegetation: Overcoming Problems in Partitioning the Diffuse Attenuation Coefficient
423 for Photosynthetically Active Radiation. *Estuaries*, **24**, 381–397.

424 Gardner TA, Cote IM, Gill JA, Grant A, Watkinson AR (2003) Long-Term Region-Wide Declines in
425 Caribbean Corals. *Science*, **301**, 958–960.

426 Giesen WBJT, Vankatwijk MM, Denhartog C (1990) Eelgrass condition and turbidity in the Dutch
427 Wadden Sea. *Aquatic Botany*, **37**, 71–85.

428 Graham NAJ, Nash KL (2013) The importance of structural complexity in coral reef ecosystems.
429 *Coral Reefs*, **32**, 315–326.

430 de Groot R, Brander L, van der Ploeg S et al. (2012) Global estimates of the value of ecosystems and
431 their services in monetary units. *Ecosystem Services*, **1**, 50–61.

432 Gurbisz C, Kemp WM (2014) Unexpected resurgence of a large submersed plant bed in Chesapeake
433 Bay: Analysis of time series data. *Limnology and Oceanography*, **59**, 482–494.

434 Halpern BS, Walbridge S, Selkoe KA et al. (2008) A global map of human impact on marine
435 ecosystems. *Science*, **319**, 948–952.

436 Jarvis JC, Moore KA (2010) The role of seedlings and seed bank viability in the recovery of
437 Chesapeake Bay, USA, Zostera marina populations following a large-scale decline.

PeerJ Preprints | https://doi.org/10.7287/peerj.preprints.2544v1 | CC BY 4.0 Open Access | rec: 21 Oct 2016, publ: 21 Oct 2016

Hydrobiologia, **649**, 55–68.

Jefferies RL, Jano AP, Abraham KF (2006) A biotic agent promotes large-scale catastrophic change in the coastal marshes of Hudson Bay. *Journal of Ecology*, **94**, 234–242.

Li X, Weller DE, Gallegos CL, Jordan TE, Kim H-C (2007) Effects of Watershed and Estuarine Characteristics on the Abundance of Submerged Aquatic Vegetation in Chesapeake. *Estuaries and Coasts*, **30**, 840–854.

Lotze HK, Lenihan HS, Bourque BJ et al. (2006) Depletion, degradation, and recovery potential of estuaries and coastal seas. *Science*, **312**, 1806–1809.

Michael Kemp W, Batleson R, Bergstrom P et al. (2004) Habitat requirements for submerged aquatic vegetation in Chesapeake Bay: Water quality, light regime, and physical-chemical factors. *Estuaries*, **27**, 363–377.

Moore KA, Jarvis JC (2008) Environmental factors affecting recent summertime eelgrass diebacks in the lower Chesapeake Bay: implications for long-term persistence. *Journal of Coastal Research*, 135–147.

Moore KA, Shields EC, Parrish DB, Orth RJ (2012) Eelgrass survival in two contrasting systems: Role of turbidity and summer water temperatures. *Marine Ecology Progress Series*, **448**, 247–258.

Najjar RG, Pyke CR, Beth M et al. (2010) Potential climage-change impacts on the Chesapeake Bay. *Estuarine, Coastal and Shelf Science*, **86**, 1–20.

NOAA Office of Science and Technology (2014) Annual Commercial Landing Statistics.

Orth RJ, Moore KA (1983) Chesapeake Bay: An unprecedented decline in submerged aquatic vegetation. *Science*, **222**, 51–53.

Orth RJ, Carruthers TJB, Dennison WC et al. (2006) A global crisis for seagrass ecosystems. *Bioscience*, **56**, 987–996.

Orth RJ, Marion SR, Moore KA, Wilcox DJ (2010) Eelgrass (Zostera marina L.) in the Chesapeake Bay region of mid-Atlantic coast of the USA: Challenges in conservation and restoration. *Estuaries and Coasts*, **33**, 139–150.

Paine DP (1981) *Aerial photography and image interpetation for resource management*.

Patrick CJ, Weller DE (2015) Interannual variation in submerged aquatic vegetation and its relationship to water quality in subestuaries of Chesapeake Bay. *Marine Ecology Progress Series*, **537**, 121–135.

Patrick CJ, Weller DE, Li X, Ryder M (2014) Effects of Shoreline Alteration and Other Stressors on Submerged Aquatic Vegetation in Subestuaries of Chesapeake Bay and the Mid-Atlantic Coastal Bays. *Estuaries and Coasts*, **37**, 1516–1531.

Patrick CJ, Weller DE, Ryder M (2016) The Relationship Between Shoreline Armoring and Adjacent Submerged Aquatic Vegetation in Chesapeake Bay and Nearby Atlantic Coastal Bays. *Estuaries and Coasts*, **39**, 158–170.

R Development Core Team (2016) R: A Language and Environment for Statistical Computing.

Ralph GM, Seitz RD, Orth RJ, Knick KE, Lipcius RN (2013) Broad-scale association between seagrass cover and juvenile blue crab density in Chesapeake Bay. *Marine Ecology Progress Series*, **488**,

PeerJ Preprints | https://doi.org/10.7287/peerj.preprints.2544v1 | CC BY 4.0 Open Access | rec: 21 Oct 2016, publ: 21 Oct 2016

51–63.

Reusch TBH, Ehlers A, Hämmerli A, Worm B (2005) Ecosystem recovery after climatic extremes enhanced by genotypic diversity. *PNAS*, **102**, 2826–2831.

van Rij J, Wieling M, Baayen RH, van Rijn H (2016) itsadug: Interpreting Time Series and Autocorrelated Data Using GAMMs.

Ruhl HA, Rybicki NB (2010) Long-term reductions in anthropogenic nutrients link to improvements in Chesapeake Bay habitat. *PNAS*, **107**, 16566–16570.

Rybicki NB, Landwehr JM (2007) Long-term changes in abundance and diversity of macrophyte and waterfowl populations in an estuary with exotic macrophytes and improving water quality. *Limnology and Oceanography*, **52**, 1195–1207.

Short FT, Wyllie-Echeverria S (1996) Natural and human-induced disturbance of seagrasses. *Environmental Conservation*, **23**, 17.

Sobocinski KL, Latour RJ (2015) Trophic transfer in seagrass systems : estimating seasonal production of an abundant seagrass fish , Bairdiella chrysoura , in lower Chesapeake Bay. *Marine Ecology Progress Series*, **523**, 157–174.

Waycott M, Duarte CM, Carruthers TJB et al. (2009) Accelerating loss of seagrasses across the globe threatens coastal ecosystems. *PNAS*, **106**, 12377–81.

Wernberg T, Bennett S, Babcock RC et al. (2016) Climate-driven regime shift of a temperate marine ecosystem. *Science*, **353**, 169–172.

Wood SN (2011) Fast stable restricted maximum likelihood and marginal likelihood estimation of semiparametric generalized linear models. *Journal of the Royal Statistical Society B*, **73**, 3–36.

PeerJ Preprints | https://doi.org/10.7287/peerj.preprints.2544v1 | CC BY 4.0 Open Access | rec: 21 Oct 2016, publ: 21 Oct 2016

498 **Table 1: Loss of ecosystem services concurrent with loss of eelgrass.** Values are means ± 1 SD,
499 estimated based on change in eelgrass cover from its peak in 1991 to present, and to the maximum
500 observed loss in 2006.

Service	Response	Present loss (1991-2015)	Maximum loss (1991-2006)
Nutrient cycling	Carbon stock (kt C)	693 ± 150	1859 ± 401
	N_2 fixation (kt N)	2.53 ± 0.25	4.25 ± 0.16
Secondary production and export	Epifaunal biomass (Mt)	141.1 ± 75.2	236.6 ± 126.1
	Blue crab density (millions of juveniles)	523 ± 600	1403 ± 1609
	Silver perch biomass (kt)	47.8 ± 5.2	80.2 ± 8.8
Total economic loss	Integrated value ($2011 US)	$1.51 billion	$2.54 billion

501

PeerJ Preprints | https://doi.org/10.7287/peerj.preprints.2544v1 | CC BY 4.0 Open Access | rec: 21 Oct 2016, publ: 21 Oct 2016

Figure Legends

Figure 1. Current (light green) and historical distribution (dark green) of eelgrass in Chesapeake Bay. Historical distribution is prior to 1971, immediately preceding Tropical Storm Agnes.

Figure 2. Thirty-year trends in eelgrass cover and distribution. (A) Total cover (hectares) has been decreasing since 1991. **(B)** Mean depth of eelgrass beds has been decreasing since 1996. **(C)** The greatest loss has occurred in the deepest beds (Deep = >0.5 m, Mid = 0-0.5 m, Shallow = 0 m). **(D)** Eelgrass has shifted 165 m closer to shore since 1984.

Figure 3. Significant predictors of eelgrass cover based on a generalized additive mixed model. (A) Predicted eelgrass cover increases with increasing Secchi depth, a measure of water clarity. Values on the y-axis represent the partial smoothed residuals accounting for the influence of the other predictors in the model. Shaded areas indicate 95% confidence intervals. **(B)** Water clarity has decreased by about 0.4 m over the past 30 years. Line denotes the predicted fit ± 95% CIs from simple linear regression. **(C)** Predicted eelgrass cover decreases with increasing summer temperature. **(D)** Mean summer temperature has increased over the past 30 years, with a more recent rise in extreme temperature events (>28 °C, triangles).

Figure 4. Interaction surface between temperature and Secchi depth from a generalized additive mixed model. Eelgrass is predicted to decline when temperature is high and Secchi depth is low (bottom right). Values on the y-axis represent the partial residuals of the tensor product (ti) smoother accounting for the influence of the other predictors in the model.

PeerJ Preprints | https://doi.org/10.7287/peerj.preprints.2544v1 | CC BY 4.0 Open Access | rec: 21 Oct 2016, publ: 21 Oct 2016

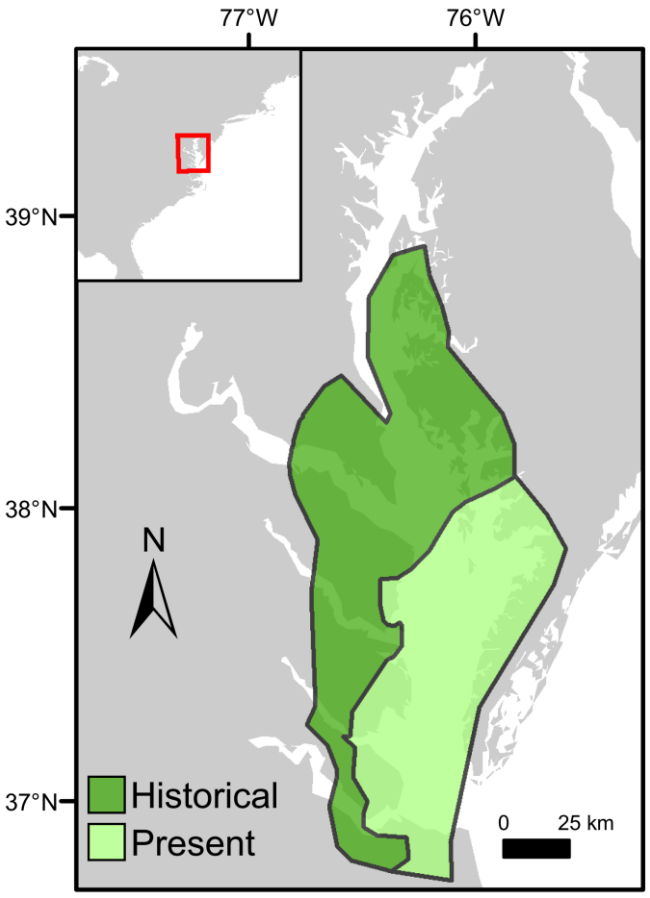

522

523 **Figure 1**

PeerJ Preprints | https://doi.org/10.7287/peerj.preprints.2544v1 | CC BY 4.0 Open Access | rec: 21 Oct 2016, publ: 21 Oct 2016

Figure 2

PeerJ Preprints | https://doi.org/10.7287/peerj.preprints.2544v1 | CC BY 4.0 Open Access | rec: 21 Oct 2016, publ: 21 Oct 2016

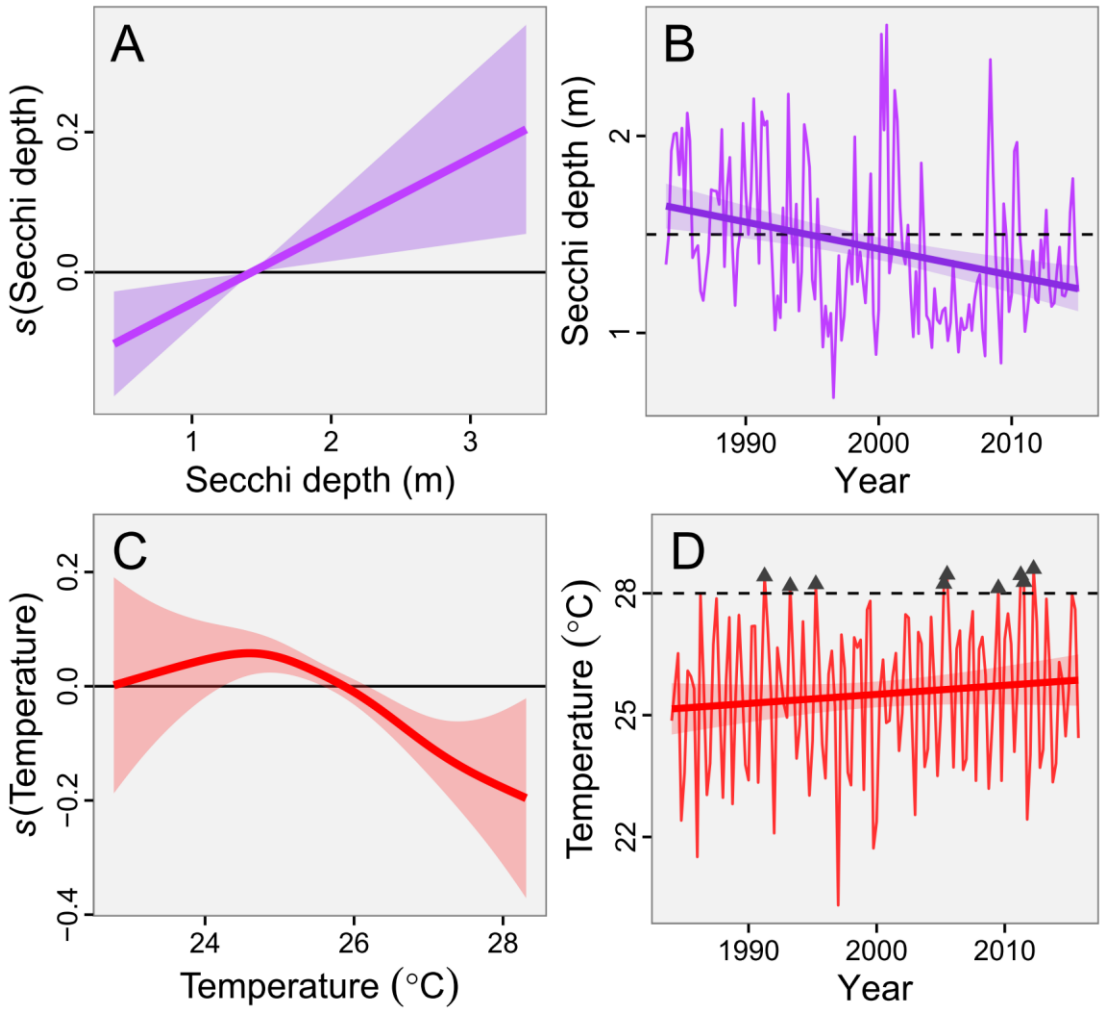

526

527 **Figure 3**

PeerJ Preprints | https://doi.org/10.7287/peerj.preprints.2544v1 | CC BY 4.0 Open Access | rec: 21 Oct 2016, publ: 21 Oct 2016

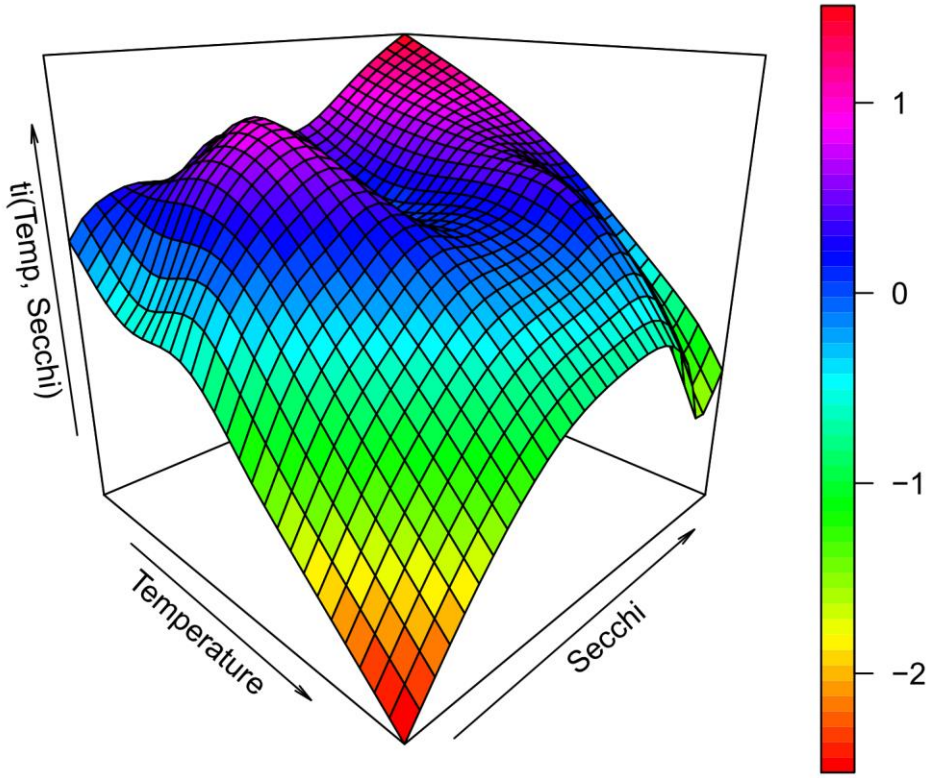

528

529 **Figure 4**

PeerJ Preprints | https://doi.org/10.7287/peerj.preprints.2544v1 | CC BY 4.0 Open Access | rec: 21 Oct 2016, publ: 21 Oct 2016

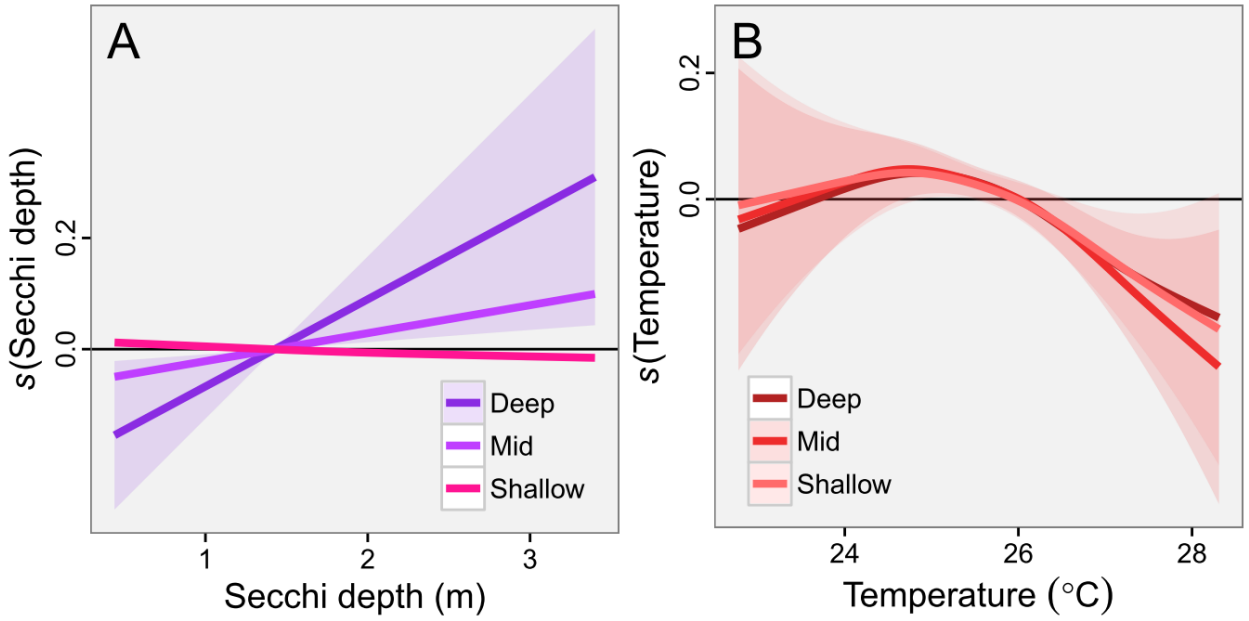

530

531 **Figure S1. Significant predictors of eelgrass cover for multiple depth strata**. Values are
532 predicted fits from generalized linear mixed effects models. Shaded areas depict 95% confidence
533 intervals, and are only shown for the significant predictors ($P < 0.05$). Deep = >0.5 m, Mid = 0-0.5 m,
534 Shallow = 0 m Mean Low Water. **(A)** Only the deepest beds (>0.5 m) had a significant relationship
535 with Secchi depth. **(B)** The intermediate and shallow beds (0-0.5 m) had a significant relationship
536 with mean water temperature of the preceding summer.

PeerJ Preprints | https://doi.org/10.7287/peerj.preprints.2544v1 | CC BY 4.0 Open Access | rec: 21 Oct 2016, publ: 21 Oct 2016

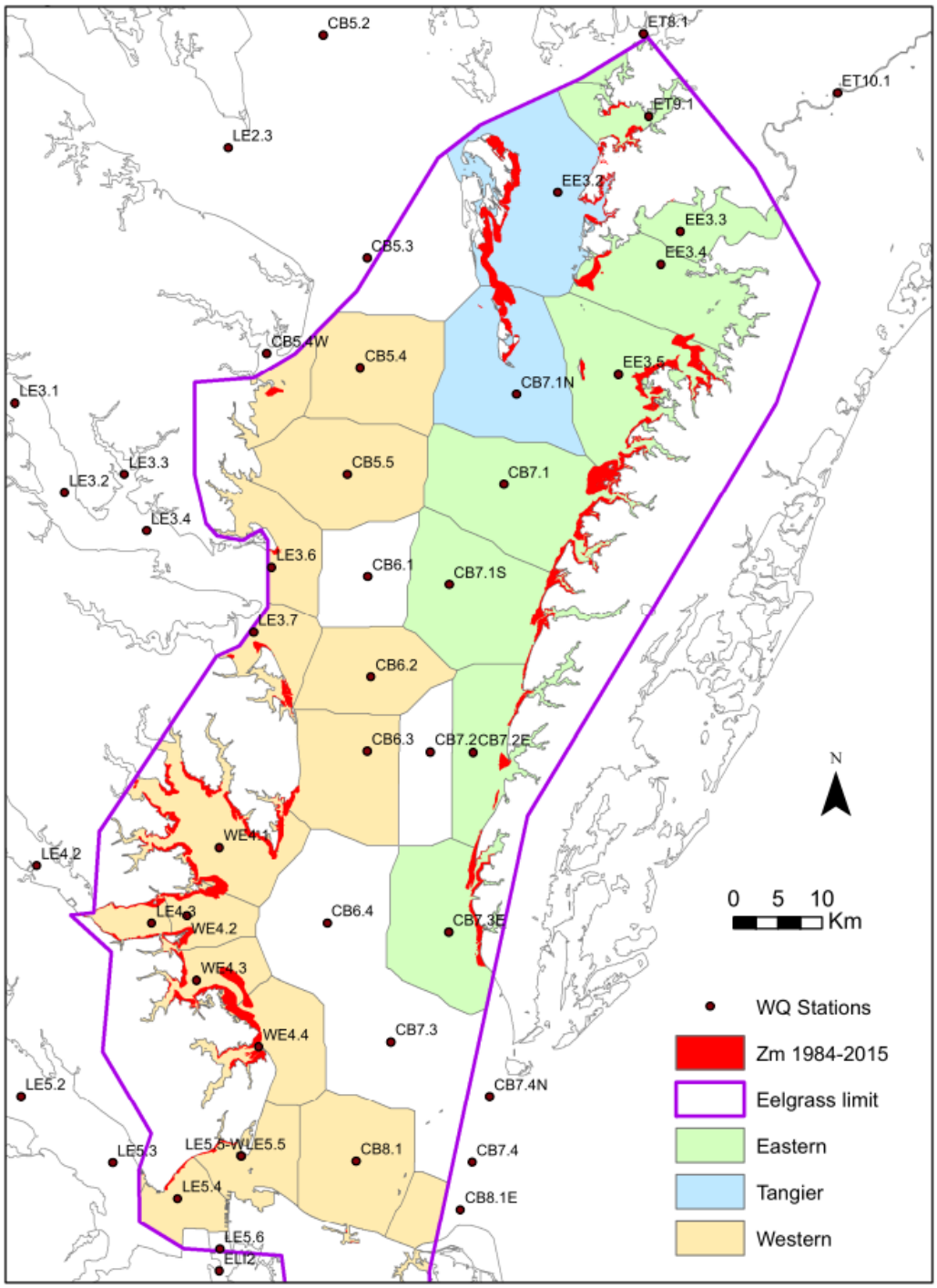

537

538 **Figure S2. The locations of eelgrass beds (red) and water quality monitoring stations (black**

539 **dots) used in the analysis.** Individual shaded polygons represent subregions used in the analysis.

540 Shading indicates the larger regions of the Chesapeake Bay used as a random effect (Eastern Shore,

541 Western Shore, Tangiers Island).

PeerJ Preprints | https://doi.org/10.7287/peerj.preprints.2544v1 | CC BY 4.0 Open Access | rec: 21 Oct 2016, publ: 21 Oct 2016